Cancer Letters 442 (2019) 222–232

Contents lists available at ScienceDirect

Cancer Letters

journal homepage: www.elsevier.com/locate/canlet

Original Articles

A novel circular RNA, circFAT1(e2), inhibits gastric cancer progression by targeting miR-548g in the cytoplasm and interacting with YBX1 in the nucleus

Jian Fang[a], Han Hong[b], Xiaofeng Xue[c], Xinguo Zhu[c], Linhua Jiang[c], Mingde Qin[d], Hansi Liang[d], Ling Gao[c,*]

[a] Department of General Surgery, Zhangjiagang Hospital Affiliated to Soochow University, Zhangjiagang, 215600, Jiangsu Province, PR China
[b] Department of Hepato-Pancreato-Biliary Surgery, Suzhou Municipal Hospital, The Affiliated Suzhou Hospital of Nanjing Medical University, Suzhou, 215000, Jiangsu Province, PR China
[c] Department of General Surgery, The First Affiliated Hospital of Soochow University, Suzhou, 215006, Jiangsu Province, PR China
[d] The Stem Cell and Biomedical Material Key Laboratory of Jiangsu Province (the State Key Laboratory Incubation Base), Soochow University, Suzhou, 215006, Jiangsu Province, PR China

ARTICLE INFO

Keywords:
Gastric cancer
circFAT1(e2)
miR-548g
RUNX1
Y-box binding protein-1 (YBX1)

ABSTRACT

In the present study, two circular RNA (circRNA) expression profiles in paired gastric cancer (GC) tissues from the GEO database were examined. We identified a novel circRNA, has_circ_0001461, which we termed circFAT1(e2). We verified that circFAT1(e2) was significantly downregulated in GC tissues and cell lines and was correlated with overall survival of GC patients. Fluorescence in situ hybridization (FISH) analysis showed that circFAT1(e2) was distributed in the cytoplasm of GC cells, as well as in the nucleus. Functional assays indicated that overexpression of circFAT1(e2) inhibited GC cell proliferation, migration and invasion. Then, we investigated whether circFAT1(e2) acts as a sponge of microRNA-549g(miR-548g) and regulates the expression of tumor suppressor RUNX1 in GC cells. Moreover, we found that nucleus-located circFAT1(e2) could directly interact with Y-box binding protein-1 (YBX1) and inhibit its function. In conclusion, circFAT1(e2) may play a role as a tumor suppressor in GC cells by regulating the miR-548g/RUNX1 axis in the cytoplasm and targeting YBX1 in the nucleus.

1. Introduction

As one of the most frequently occurring gastric diseases, gastric cancer (GC) is considered to be the most serious threat to the health and even the life of patients [1,2]. Although diagnosis and therapy technologies have been developing rapidly, the prognosis of GC is still poor in recent years [3,4]. A lack of effective diagnostic measures and biomarkers for GC may be the most important reason [5]. Therefore, elucidating the underlying molecular mechanisms of GC initiation and progression is extremely necessary for the screening of proper biomarkers and the development of effective therapeutic measures for GC patients.

Noncoding RNAs (ncRNAs), including microRNAs (miRNAs), long noncoding RNAs (lncRNAs), and circular RNAs (circRNAs), were initially considered to be meaningless for the development of GC [6–8]. However, with more and more research available, the functions of ncRNAs have begun to change from a useless type of RNA to an important gene regulator [6,9,10]. A vast amount of studies have demonstrated that ncRNAs may be involved in the tumorigenesis of many human tumors, such as breast cancer, lung cancer, and liver cancer, by controlling the expression of oncogenes and tumor suppressor genes [11–13]. In particular, circRNAs, which are characterized by covalently closed continuous loops without 5′ to 3′ polarity and a polyadenylated tail, were revealed to exert regulatory effects on gene expression in many human cancers [14,15]. They were proven to function as competing endogenous RNAs to regulate miRNA levels and affect the targeted gene expression [16,17]. However, the roles of circRNAs in the progression of GC are still largely unknown.

In our study, we analyzed the data of two independent microarray datasets (GES100170 and GSE83521) from the Gene Expression Omnibus database and identified that circFAT1(e2) was significantly downregulated in GC tissues and cell lines and predicted a better

* Corresponding author. Department of General Surgery, The First Affiliated Hospital of Soochow University, No. 188 Shizi Street, Suzhou, 215006, Jiangsu Province, PR China.
E-mail address: gaol0614@sohu.com (L. Gao).

https://doi.org/10.1016/j.canlet.2018.10.040
Received 19 June 2018; Received in revised form 20 October 2018; Accepted 25 October 2018

prognosis of GC patients. We found that circFAT1(e2) was distributed not only in the cytoplasm of GC cells but also in the nucleus. The circFAT1(e2) circRNA could inhibit GC tumor growth by acting as a sponge of miR-548g in the cytoplasm and binding to the YBX1 protein in the nucleus. Hence, circFAT1(e2) may serve as an effective inhibitor and biomarker for GC therapy and diagnosis.

2. Materials and methods

2.1. Patient tissue samples and cell lines

Fresh-frozen GC tissues and corresponding normal gastric epithelial tissues were collected from 38 patients who underwent tumor surgical resection at The First Affiliated Hospital of Soochow University from May 2015 to May 2018. The study was approved by the ethics committee of The First Affiliated Hospital of Soochow University and informed consents were provided by all patients. The normal human gastric epithelial mucosa cell line (GSE-1), and human GC cell lines (SGC-7901, BGC-823, MKN-28, AGS, MGC-803, and MKN-45) were all purchased from the Culture Collection of Chinese Academy of Sciences (Shanghai, China). All cells were maintained and stored following the instructions obtained from their providers. Briefly, MGC-803, BGC-823, MKN-28, SGC-7901 cells were maintained in RPMI-1640 medium GES-1 and HEK-293T cells were maintained in Dulbecco's modified Eagle's medium (Gibco, Grand Island, NY, USA). AGS and DMEM/F12 medium cells were cultured in DMEM/F12 medium (ThermoFisher; Cat. No. 11330-057). All medium were supplemented with 10% fetal bovine serum (FBS, Gibco), 2 mM L-glutamine, penicillin and streptomycin (Gibco BRL, NY, USA). All cell lines were cultured in humidified air supplemented with 5% CO_2 at 37 °C.

2.2. circRNAs expression profile analysis

Two gene expression profiles (GES100170 and GSE83521) of GC were downloaded from the Gene Expression Omnibus database (GEO, http://www.ncbi.nlm.nih.gov/geo). GSE100170 consisted of 10 samples, including 5 normal samples and 5 GC samples. GSE83521 include 12 samples, consisting of 6 normal mucosa tissue samples and 6 GC tissue samples. GEO2R (http://www.ncbi.nlm.nih.gov/geo/geo2r/), an online analysis tool, was used to compare the differentially expressed genes (DEGs) of GES100170 and GSE83521 in our study. The adjusted P values were used to correct for the occurrence of false positive results via the Benjamini and Hochberg false discovery rate method.

2.3. RNase R resistance analysis of circRNAs

The circFAT1(e2) from MGC-803 cells was treated with RNase R (4 U/mg, Epicenter) or actinomycin D and incubated for 30 min at 37 °C. Then, the treated RNAs were reverse transcribed with specific primers and detected by quantitative real-time PCR (qRT-PCR) assay.

2.4. RNA extraction and quantitative real-time PCR (RT-PCR) assay

The total RNA of the GC tissues/cell lines and corresponding normal tissues/cell lines were extracted by TRIzol reagent (Invitrogen, Carlsbad, CA, USA) following the manufacturer's instructions. After RNA quantification and quality examination by NanoDro2000c (Thermo Scientific, Waltham, USA), 2 μg of total RNA were reverse transcribed to cDNA via BestarTM qPCR RT kit (#2220, DBI Bioscience, China). Then, the quantitative polymerase chain reaction (RT-PCR) assay was conducted using BestarTM qPCR MasterMix (#2043, DBI Bioscience, China) on an ABI7500 according to the protocols obtained from the manufacturers. The primers used in this study are listed in Table 1. All primers were designed and purchased from Sangon, China; the mRNA expression of miR-548g was normalized to U6, and the mRNA expression of EGFP, c-Met, and CDC25A were normalized to GAPDH.

2.5. Fluorescence in situ hybridization (FISH)

In situ hybridization was carried out using specific probes to the circFAT1(e2) sequence. Biotin-labeled specific RNA probes were transcribed from circFAT1(e2) PCR fragments using the biotin-labeling mix and RNA polymerase (Roche, China) according to the instructions provided by manufacturers. After grown to the exponential phase, MGC-803 cells were fixed using 4% formalin. Tissues were cut into 4 μm sections and then also fixed with 4% formalin. Cells and tissues were then hybridized in hybridization buffer with biotin-labeled probes specific to circFAT1(e2). Signals were measured by a tyramide-conjugated Alexa 488 fluorochrome TSA kit. The results were obtained by using a Laser Scanning Confocal Microscope (Leica, Germany) at 400 x magnification.

2.6. In vivo tumor formation assay

Male BALB/c mice (six weeks old) were obtained from the Institute of Zoology, Chinese Academy of Sciences, and the animal studies were approved by the Institutional Animal Care and Use Committee of Soochow University. MGC-803 cells transfected with circFAT1(e2) or NC were harvested from 6-well plates, washed with phosphate-buffered saline (PBS), and then resuspended with medium at 2×10^6 cells/mL. Subsequently, 100 μL of suspended MGC-803 cells were injected into the left flank of nude mice. Tumor growth was examined at 0, 7, 21, 28 days after injection; volumes of tumors were measured as the length × width^2 × 0.5.

2.7. Ki-67 staining

GC tumor tissues were collected from xenografts in nude mice, fixed with 10% formalin, embedded in paraffin and cut into 4 μm sections. Tissues sections were incubated with primary antibodies against Ki-67 (Rabbit, 1:50, ab833, Abcam) overnight at 4 °C. Tissues were then incubated with secondary antibodies (Goat anti Rabbit, 1:1000, ab6721, Abcam) for 2 h at room temperature.

2.8. Statistical analysis

Data in this present study were all expressed as the mean ± SEM. All statistical analyses were carried out using GraphPad (Ver. Prism 7, GraphPad Prism Software, La Jolla, CA, USA) and SPSS 20.0 (IBM, SPSS, Chicago, IL, USA). According to Benjamini and Hochberg, the false discovery rate may be the appropriate error rate to control in many applied multiple testing problems [18]. The two-tailed Student's t-test was used for the analysis of continuous variables. We determined the differences among the three groups by using a nonrepeated measures ANOVA and Scheffe's test. A P value less than 0.05 was considered significant. More detailed Materials and Methods are included in the supplementary file.

3. Results

3.1. Hsa_circ_0001461 (circFAT1(e2)) was identified as a GC related circular RNA

To identify the circRNAs involved in GC tumorigenesis, we first searched the GEO database with “circRNA” and “gastric cancer”; the results showed that there were six GSE datasets (Table S1), and GSE100170 and GSE83521 were chosen randomly for further study. We identified 250 up/down regulated circRNAs in GSE100170 or GSE83521 (Fig. 1A and supplementary Excel-1 and Excel-2). Among them, the hsa_circ_0006089 (logFC = 65.27389, P = 0.006806), hsa_circ_0004339 (logFC = 39.83934, P = 0.005029) and

Table 1
Primer and sequence in this study.

GENE	Primer	
	Forward (5′-3′)	Reverse (5′-3′)
GAPDH	TGTTCGTCATGGGTGTGAAC	ATGGCATGGACTGTGGTCAT
circFAT1	AACAGAAGAGAACTGGGGCG	GATCAGGGTGCCAATGGTGA
miR-548g	ACACTCCAGCTGGGTGCAAAAGTAATTGCAG	CTCAACTGGTGTCGTGGAGTCGGCAATTCAGTTGAGCAAAAACT
U6	CTCGCTTCG GCAGCACA	AACGCTTCACGAATTTGCGT
EGFR	CCAACTATGGGACAAACAGAA	ATCGCACAGCACCAATCA
CDC25A	TCTGAAGAATGAGGAGGAGAC	AAA CAG CTT GCA TCG GTT GT
c-Met	TATGTGGCTGGGACTTTGGA	GCT TATTCATGG CAG GACCAA C

hsa_circ_0045602 (logFC = 25.81513 P = 0.007401) were highest in GSE100170; the hsa_circ_0018004 (logFC = 0.329614, P = 0.000792), hsa_circ_0071681 (logFC = 0.328798, P < 0.001) and hsa_circ_0032832 (logFC = 0.317411, P = 0.027136) were lowest in GSE100170 (Fig. 1A and supplementary Excel-1). The hsa_circ_0084717 (logFC = 23.97234, P = 0.030952, hsa_circ_0058145 (logFC = 10.2277, P = 0.032133) and hsa_circ_0044516 (logFC = 9.374326, P = 0.0109) were highest in GSE83521; the hsa_circ_0000583 (logFC = 0.059271, P = 0.005288), hsa_circ_0076304 (logFC = 0.046037, P = 0.001511) and hsa_circ_0035431 (logFC = 0.043576, P = 0.000249) were lowest in GSE83521 (Fig. 1A and supplementary Excel-2). Only two circRNAs were consistently downregulated in both datasets: hsa_circ_0067997 and hsa_circ_0001461 (Fig. 1B). RT-PCR analysis of hsa_circ_0067997 showed no products in MGC-803 cells with divergent primers (Fig. S1A). Therefore, we chose hsa_circ_0001461 for further research. Hsa_circ_0001461, which was termed circFAT1(e2), arose from the FAT1 gene and consisted of the head-to-tail splicing of exon 2 (Fig. 1C). We designed convergent primers to amplify linear mRNA of exon 10 from FAT1 (linFAT1), as well as divergent primers to amplify circFAT1(e2), to validate the formation of circFAT1(e2). Using cDNA and gDNA as templates, circFAT1(e2) could only be amplified by divergent primers in cDNA, and no products were observed in the gDNA groups (Fig. 1D). Then, the RT-PCR product of circFAT1(e2) was confirmed by Sanger sequencing (Fig. 1E). Moreover, fluorescence in situ hybridization (FISH) against circFAT1(e2) revealed that circFAT1(e2) were not only localized in the cytoplasm but also in the nucleus (Fig. S1B). Actinomycin D and RNase R exonuclease were used to further validate circFAT1(e2) in MGC-803 cells. Resistance to actinomycin D and RNase R exonuclease confirmed that this RNA species was indeed circular (Fig. 1F and G). We also confirmed the presence of circFAT1(e2) by actinomycin D and RNase R exonuclease in MKN-28 cells ($P < 0.05$, Figs. S1C and 1D).

3.2. CircFAT1(e2) expression was downregulated in GC tissues and cell lines and predicted better prognosis

To explore the functions of circFAT1(e2) in GC, we first examined its expression in GC tissues and cell lines by RT-PCR analysis. It was demonstrated that circFAT1(e2) expression was significantly downregulated in GC tissues compared to normal tissues (Fig. 2A), and its expression was lower in metastasis tissues (n = 7) than non-metastasis tissues (n = 31) ($P < 0.05$, Fig. 2B). Moreover, circFAT1(e2) expression was remarkably decreased in six GC cell lines compared with the normal human gastric epithelial mucosa cell line GES-1 (Fig. 2C). FISH was used to further evaluate the expression of circFAT1(e2), and results showed that its expression was significantly lower in GC tumor tissues than in normal tissues ($P < 0.05$, Fig. 2D and E). There was no correlation between circFAT1(e2) expression and age, or gender. However, circFAT1(e2) expression was significantly correlated with the pN status, pM status and clinical stage ($P < 0.05$, Table S2).

3.3. Overexpression of circFAT1(e2) significantly inhibited GC cell proliferation, invasion, and migration

To explore the functions of circFAT1(e2) in GC cells, we established a recombinant plasmid containing the exon2 of FAT1 and CMV promoter to generate GC cell lines that stably overexpressed circFAT1(e2) (Fig. 3A). The relative expression of circFT1 was significantly increased in transfected MGC-803 and MKN-28 cells ($P < 0.05$, Fig. 3B). Cell growth curves demonstrated that overexpression of circFAT1(e2) significantly inhibited cell proliferation in MGC-803 and MKN-28 cells (Fig. 3C and D). Colony formation assay suggested that overexpression of circFAT1(e2) remarkably reduced the number of colonies of MGC-803 and MKN-28 cells ($P < 0.05$, Fig. 3E-H). Moreover, transwell assays indicated that overexpression of circFAT1(e2) significantly attenuated the invasive and migratory abilities of MGC-803 and MKN-28 cells ($P < 0.05$, Figs. S2A–2D). We further explored the effects of enforced expression of circFAT1(e2) on regulating tumor growth *in vivo*. MGC-803 cells stably transfected with circFAT1(e2) or NC were subcutaneously injected into BALA/c mice, the tumor volume and weight were measured 0, 7, 14, 21, and 28 days after injection. Decreased tumor volume and weight of the xenografts were revealed in circFAT1(e2) transfectants compared with the NC group ($P < 0.05$, Fig. 3I-K). Immunohistochemistry (IHC) analysis suggested that the tumors formed from circFAT1(e2) transfected MGC-803 cells exhibited weaker Ki-67 staining than the tumors derived from NC transfected cells ($P < 0.05$, Fig. 3L).

3.4. circFAT1(e2) upregulated RUNX1 expression by directly binding to miR-548g in GC cell lines

To address the subcellular location of circFAT1(e2) in MGC803 cells, RT-PCR and FISH were performed in our study. The results showed that circFAT1(e2) was localized in both the cytoplasm (55%) and nucleus (45%) in MGC-803 cells ($P < 0.05$, Fig. 4A and S1B). It has been demonstrated that circRNAs may serve as competing RNAs to bind miRNAs in the cytoplasm. Therefore, we speculated that circFAT1(e2) may target miRNAs in MGC-803 cells. The circFAT1(e2)-miRNAs interaction analysis based on TargetScan (http://www.targetscan.org/vert_71/) showed the predicted targeted miRNAs of circFAT1(e2) in MGC-803 cells (Supplementary Excel-3) and that miR-548g had five binding sites for circFAT1(e2) (Fig. 4B). To validate the interaction between miR-548g and circFAT1(e2), wild type or mutant targeted sites of miR-548g in circFAT1(e2) were cloned into pGL3. Results from the dual luciferase reporter assay indicated that miR-548g mimics significantly attenuated the luciferase activity driven by wild type circFAT1(e2) ($P < 0.05$, Fig. 4C). Additionally, miR-548g inhibitors remarkably enhanced the luciferase activity driven by wild type circFAT1(e2) ($P < 0.05$, Fig. 4D), whereas the mutant circFAT1(e2) was not affected by miR-548g. RNA precipitation (RIP) was performed to further determine the interaction between miR-548g and circFAT1(e2) using a miR-548g specific probe. As expected, we found a specific enrichment of circFAT1(e2) and miR-548g in the miR-548g

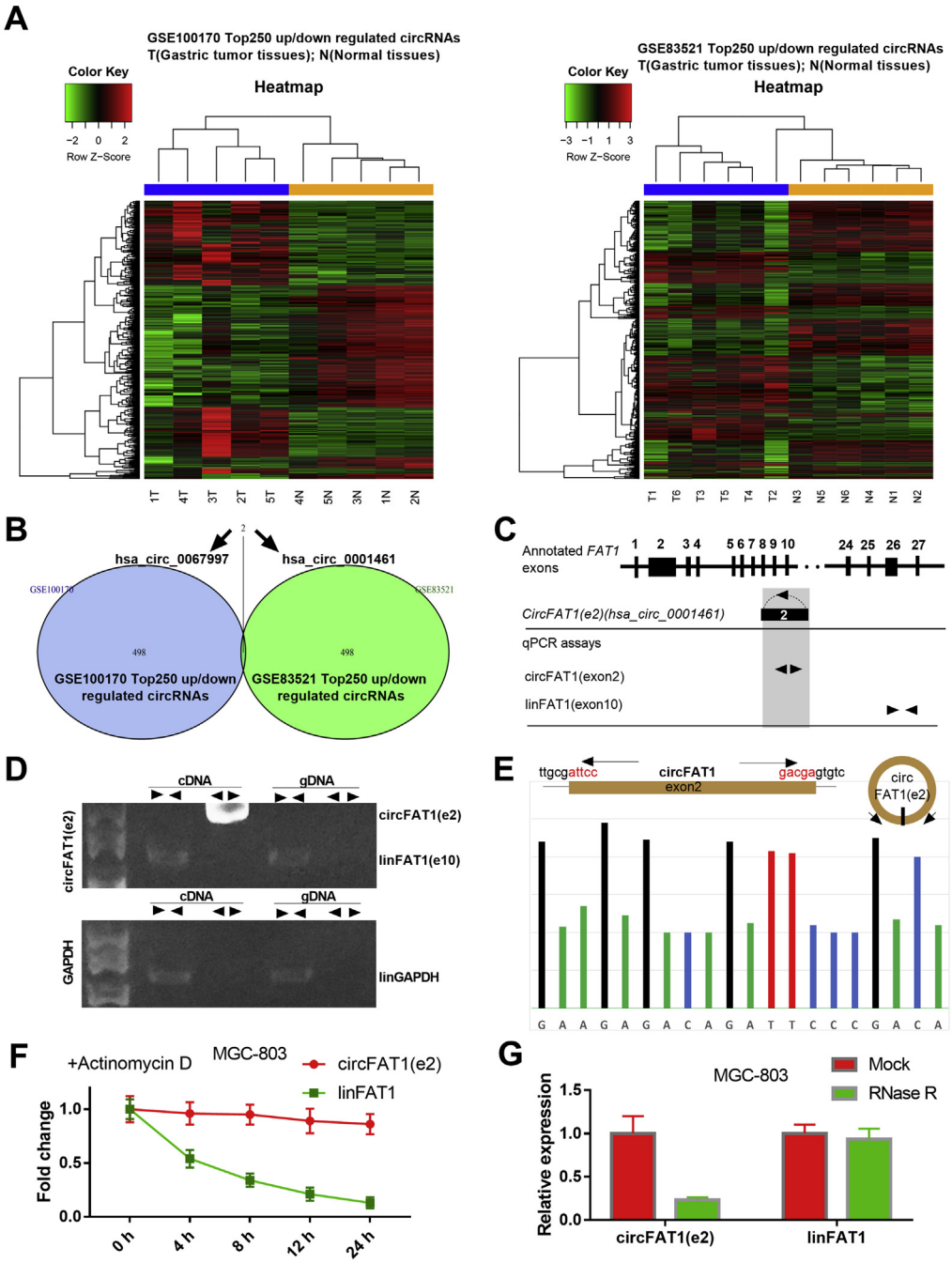

Fig. 1. Identification of hsa_circ_0001461 [circFAT1(e2)] as a GC related circRNA. (A) Hierarchical clustering analysis of circRNAs that were differentially expressed in gastric tumor tissues and normal tissues in GSE100170 (left) and GSE83521 (right). **(B)** Overlap of dysregulated circRNAs in GSE100170 and GSE83521. **(C)** Schematic diagram of the genomic location of circFAT1(e2). **(D)** CircFAT1(e2) was validated by RT-PCR using divergent primers in cDNA and gDNA. **(E)** Sanger sequencing of circFAT1(e2) showed the back-splice junction. **(F)** RT-PCR analysis of circFAT1(e2) and linFAT1 in MGC-803 cells treated with actinomycin. **(G)** RT-PCR analysis of circFAT1(e2) and linFAT1 in MGC-803 cells treated with RNase R. The expression of circFAT1(e2) and linFAT1 were normalized to the value detected in the mock group.

specific probe group compared with the scramble group ($P < 0.05$, Fig. 4E). Moreover, we found that the miR-548g-specific probe could only pull down circFAT1(e2) in the cytoplasm, rather than the nucleus, of MGC-803 ($P < 0.05$, Fig. 4H). These findings suggested that circFAT1(e2) may directly bind to miR-548g in the cytoplasm of MGC-803 cells.

To further confirm the correlation between circFAT1(e2) and miR-548g, we established circFAT1(e2) overexpressed and blocked cell models by transfecting MGC-803 cells with circFAT1(e2) and si-circFAT1(e2), respectively. We designed three siRNAs against circFAT1(e2) (Fig. S3A), and siRNA-1 showed the best knockdown efficiency of circFAT1(e2) in SGC7901 cells ($P < 0.05$, Fig. S3B). Thus, siRNA-1 (si-circFAT1(e2)) was used to block circFAT1(e2) expression and validated in SGC7901 and AGS cells ($P < 0.05$, Fig. S3C). RT-PCR analysis showed a significant decrease of miR-548g in MGC-803 cells transfected with circFAT1(e2) ($P < 0.05$, Fig. 4F) and displayed a remarkable increase of miR-548g in MGC-803 cells transfected with si-circFAT1(e2) ($P < 0.05$, Fig. 4G). Analysis of circFAT1(e2) and miR-548g copy numbers in six GC cell lines showed a negative correlation between circFAT1(e2) and miR-548g (Fig. 4I). These results indicated

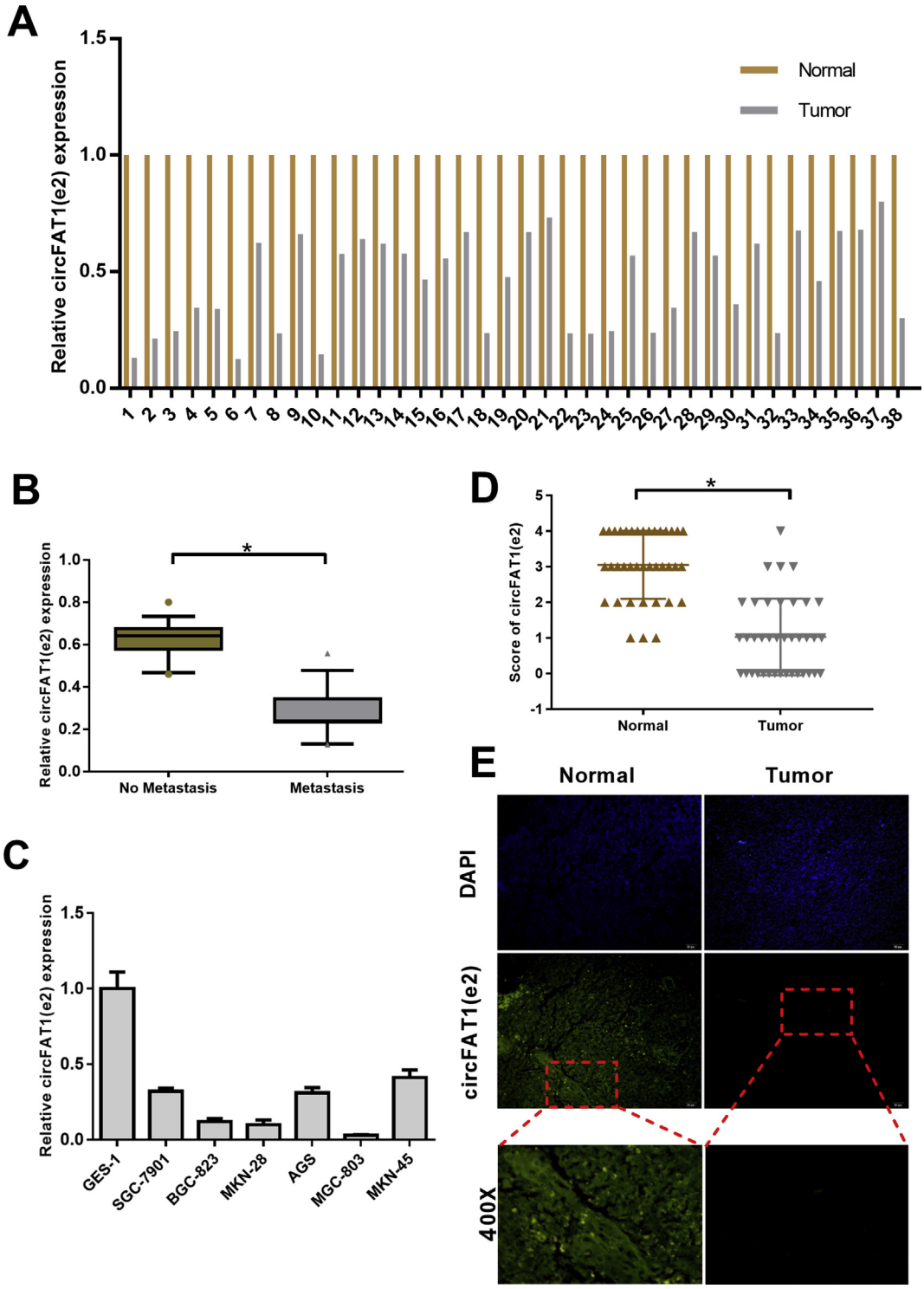

Fig. 2. circFAT1(e2) was frequently downregulated in GC and predicted better prognosis. (A) Relative expression of circFAT1(e2) from 38 pairs of normal tissues and GC tissues measured by RT-PCR. **(B)** Relative expression of circFAT1(e2) from metastasis and non-metastasis GC tissues detected via RT-PCR. $P < 0.05$. **(C)** Relative expression of circFAT1(e2) from six GC cell lines (SGC-7901, BGC-823, MKN-28, AGS, MGC-803, and MKN-45) and one normal human gastric epithelial mucosa cell line (GSE-1) by RT-PCR. **(D)** Statistical chart (n = 38, $P < 0.05$) and **(E)** representative images of circFAT1(e2) from normal tissues and GC tissues determined by fluorescence in situ hybridization (FISH).

that circFAT1(e2) could negatively regulate the expression of miR-548g in GC cells.

3.5. miR-548g promoted GC cell tumorigenesis partly though RUNX1

Bioinformatics analysis showed three binding sites for miR-548g in the 3′-UTR of RUNX1 (Fig. 5A). We then evaluated the interaction between miR-548g and RUNX1 by dual-luciferase reporter assay ($P < 0.05$, Fig. 5B). In addition, Western blot assay showed that RUNX1 expression was significantly higher in circFAT1(e2) transfected MGC-803 and MKN-28 cells than in cells treated with NC (Fig. 5C). RUNX1 expression was obviously lower in si-circFAT1(e2) transfected

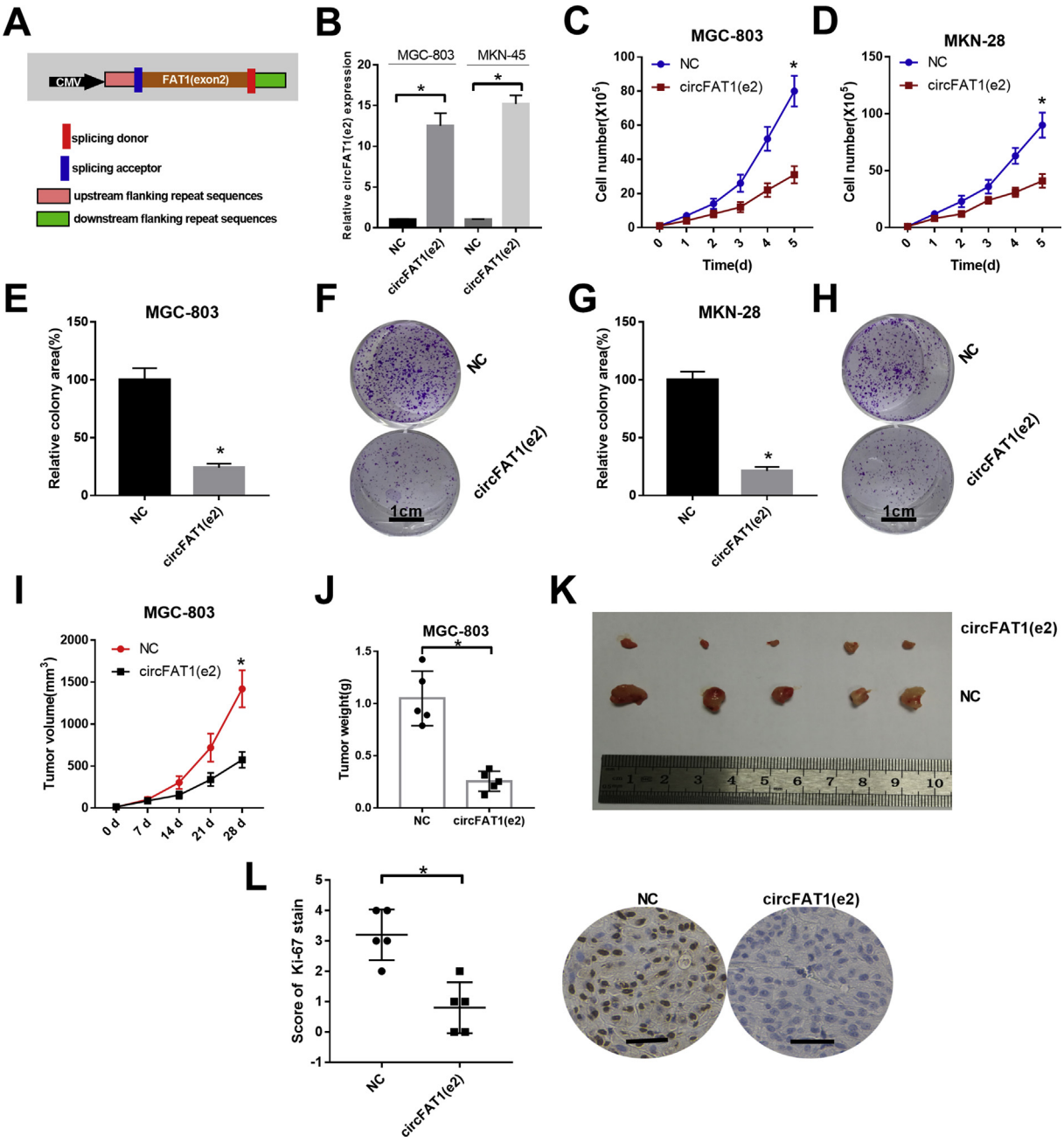

Fig. 3. CircFAT1(e2) was an important tumor suppressor for GC cell survival and proliferation. (A) Schematic diagram of the cicrFAT1 overexpression vector. **(B)** The transfection efficiency of cicrFAT1 was evaluated by RT-PCR in MGC803 and MKN-45 GC cell lines, $P < 0.05$. **(C and D)** Growth curves of MGC-803 and MKN-28 cells transfected with circFAT1(e2) or negative control (NC), $P < 0.05$. A colony formation assay was performed to measure the cell proliferation of MGC-803 cells **(E and F)** and MKN-28 cells **(G and H)** transfected with circFAT1(e2) or NC, $P < 0.05$. **(I-K)** Hypodermic injection of MGC-803 cells transfected with circFAT1(e2) or NC into BALB/c nude mice established the xenograft model; tumor volume and weight were measured, $P < 0.05$. **(L)** Immunohistochemical analysis of Ki-67 expression in tissues from xenograft, $P < 0.05$.

SGC-7901 and AGS cells than those cells treated with si-NC (Fig. 5D). RUNX2 and RUNX3 expression were not affected by circFAT1(e2) overexpression and knockdown in GC cells. Further exploration of RUNX1 expression revealed that miR-548g could reverse the upregulation of RUNX1 induced by circFAT1(e2) in MGC-803 and MKN-28 cells (Fig. 5E). Taken together, our findings demonstrated that circFAT1(e2) could upregulate RUNX1 expression by miR-548g.

Cell growth curves suggested that overexpression of miR-548g significantly promoted cell growth, and miR-548g could abolish the downregulation of cell growth induced by RUNX1 in MGC-803 and MKN-28 cells ($P < 0.05$, Fig. 5F and G). Colony formation assays showed a significantly higher number of colonies in miR-548g overexpressed GC cells, and overexpression of miR-548g reversed the reduction of the number of colonies induced by RUNX1 (Fig. 5H and I). Moreover, we found that overexpression of miR-548g significantly increased the invasive ability of MGC-803 cells. However, overexpression of RUNX1 remarkably decreased the invasive ability of MGC-803 cells, and miR-548g could partly abolish the effects induced by overexpression of RUNX1 ($P < 0.05$, Figs. S4A and S4B). These results indicated that miR-548g could promote GC tumorigenesis through RUNX1.

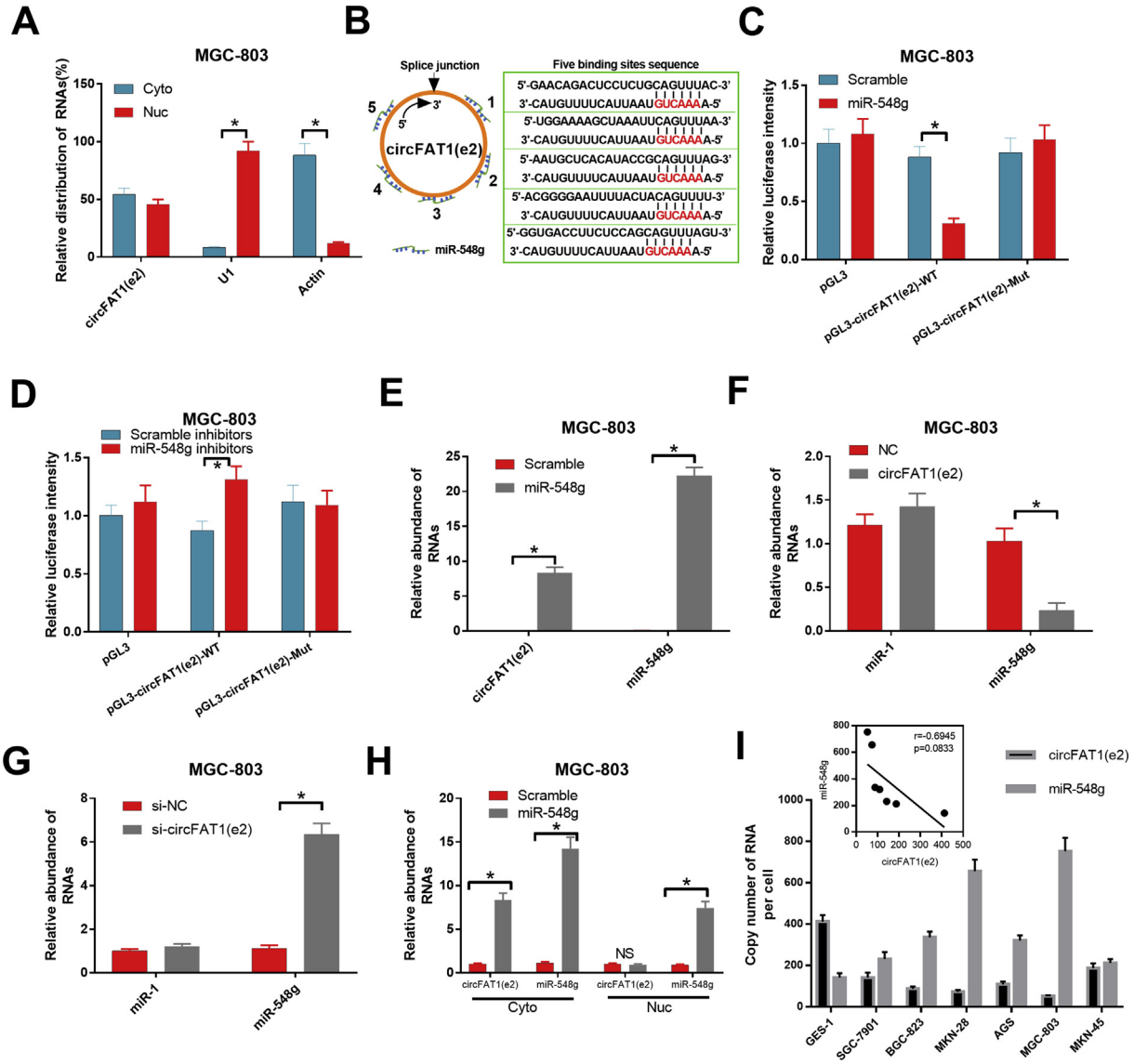

Fig. 4. circFAT1(e2) sequestered miR-548g to stabilize RUNX1. (A) Relative distribution of circFAT1(e2) in MGC-803 cells. **(B)** The putative sequence of miR-548g and circFAT1(e2) with five binding sites. **(C and D)** Interaction between miR-548g and circFAT1(e2) was determined by luciferase reporter assay in MGC803 and MKN-28 cells. **(E)** RIP assay was carried out to determine the interaction between circFAT1(e2) and miR-548g using a specific miR-548g probe or scramble in MGC-803 cells, $P < 0.05$. Relative expression of miR-548g was assessed in **(F)** circFAT1(e2) overexpressed and **(G)** circFAT1(e2) knockdown MGC-803 cells by RT-PCR; miR-1 expression was used as negative control, $P < 0.05$. **(H)** RIP assay was used to further determine the interaction between miR-548g and circFAT1(e2) in the cytoplasm and nucleus of MGC-803 cells via a specific miR-548g probe, $P < 0.05$. **(I)** Correlation between circFAT1(e2) and miR-548g in six GC cell lines and one normal human gastric epithelial mucosa cell line.

3.6. circFAT1(e2) directly bind to Y-box binding protein-1 (YBX1)

Results from above study revealed that circFAT1(e2) are distributed in the cytoplasm and nucleus of GC cells, and cytoplasmic circFAT1(e2) was demonstrated to play a role as a GC inhibitor by interacting with miR-548g. However, whether nuclear circFAT1(e2) participates in the tumorigenesis of GC remains undetermined. Using the online catRAPID algorithm, we found multiple proteins that may be bound by circFAT1(e2) (Table S3). First, among these proteins, YBX1 got the highest score. Second, YBX1 plays important roles in GC with multi-ncRNAs, so it was chosen for further exploration. CircFAT1(e2) was artificially divided into four parts (a, 1-1000; b, 1001-2000; c, 2001-3000; d, 3001-3283). These four parts were subjected to catRAPID to analyze the interaction with YBX1 protein; part a (1-1000) and part d (3001-3283) showed higher scores (Fig. 6A). We then conducted RNA immunoprecipitation (RIP) in MGC-803 cells to pull down circFAT1(e2) using an anti-YBX1 antibody, followed by RT-PCR analysis and Western blot assay for circFAT1(e2) expression. The results showed that circFAT1(e2) expression was significantly higher in the anti-YBX1 group than the IgG group ($P < 0.05$, Fig. 6B). Moreover, the four parts of circFAT1(e2) were transcribed *in vitro* and then served as anchors to pull down YBX1 in cell nucleus lysate, respectively. Western blot assay showed a specific enrichment of YBX1 in part a and part d groups (Fig. 6C). These results showed that circFAT1(e2) specifically interacted with YBX1 in GC cells.

3.7. circFAT1(e2) inhibited GC cell tumorigenesis through YBX1

RT-PCR analysis demonstrated that overexpression of circFAT1(e2) significantly downregulated the expression of three targeted genes of YBX1 (EGFP, c-Met, and CDC25A). However, YBX1 could abolish this effect induced by circFAT1(e2) in MGC-803 and MKN-28 cells ($P < 0.05$, Fig. 7A and B). Cell growth curve analysis showed that overexpression of circFAT1(e2) in MGC-803 and MKN-28 cells could

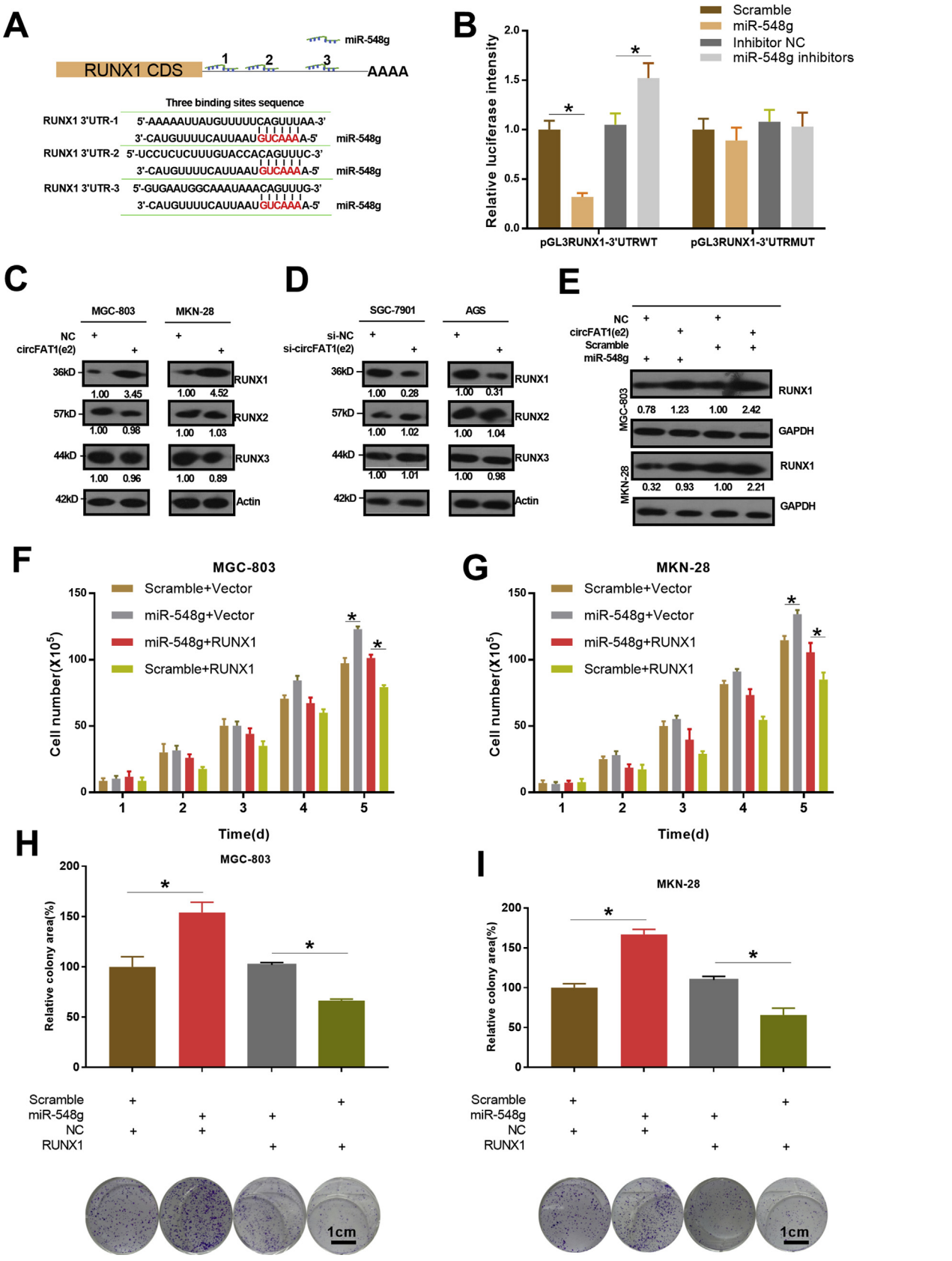

Fig. 5. miR-548g promoted GC cell tumorigenesis partly though RUNX1. (A) The putative sequences of miR-548g and RUNX1 with three binding sites. **(B)** Interaction between miR-548g and RUNX1 was validated by luciferase reporter assay, $P < 0.05$. **(C and D)** Western blot analysis of RUNX1, RUNX2, and RUNX3 expression in MGC-803, MKN-28, SGC-7901, and AGS cells transfected with circFAT1(e2) or NC. **(E)** Western blot analysis of RUNX1 in MGC-803 and MKN-28 cells transfected with circFAT1(e2) or miR-548g. **(F and G)** Cell number of MGC-803 and MKN-28 cells treated with miR-548g mimics or RUNX1 was determined by MTT assay at 1, 2, 3, 4, and 5 days after transfection, $P < 0.05$. **(H and I)** Colony formation assay was performed to assess the cell proliferation of MGC-803 and MKN-28 cells treated with miR-548g mimics or RUNX1, $P < 0.05$.

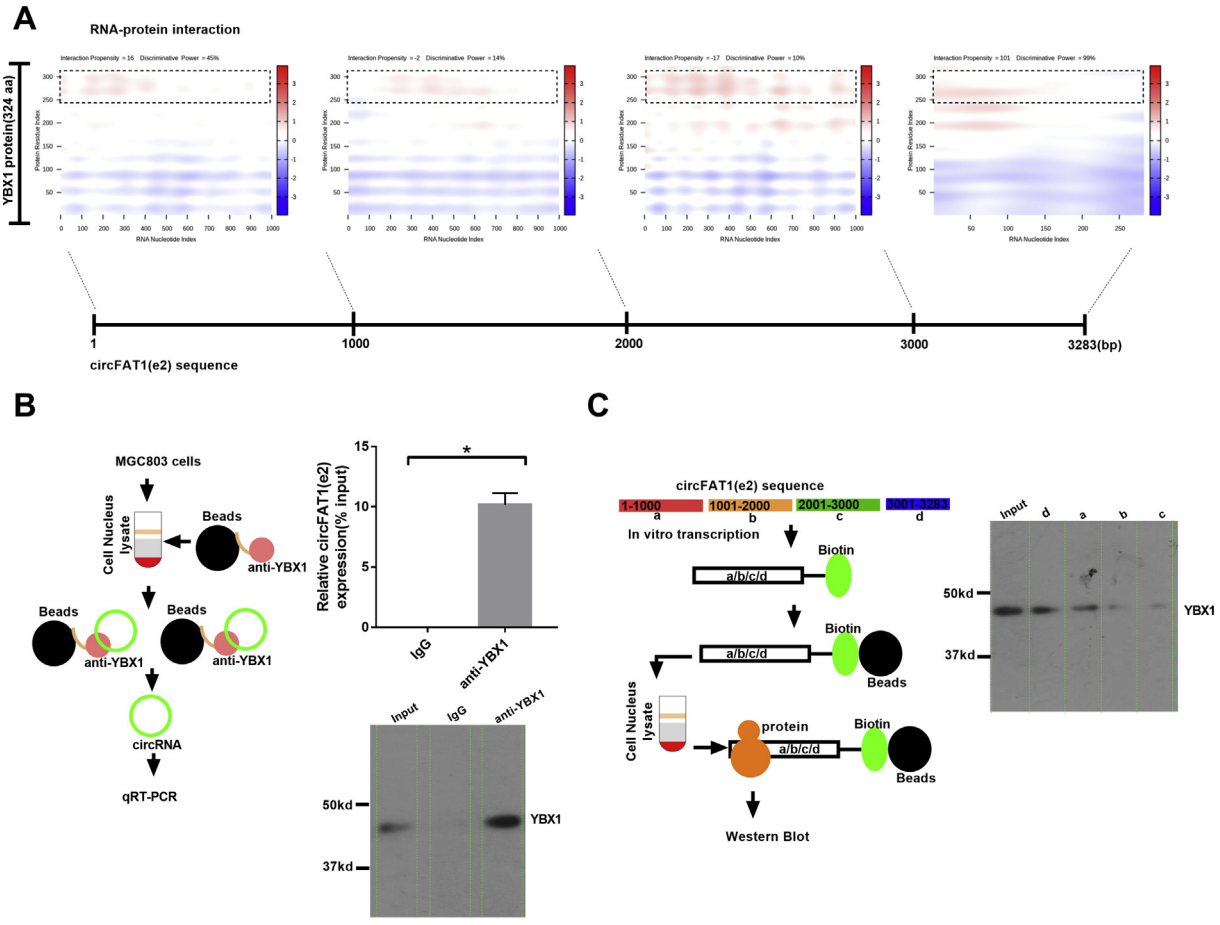

Fig. 6. circFAT1(e2) directly bind to YBX1. (A) The catRAPID algorithm was applied to predict the RNA-protein interaction of circFAT1(e2) and YBX1. **(B and C)** The interaction between circFAT1(e2) and YBX1 was validated by RNA immunoprecipitation (RIP) in MGC-803 cells.

significantly reduce the cell number, however, YBX1 could abolish the reduction of cells induced by circFAT1(e2) overexpression ($P < 0.05$, Fig. 7C and D). Colony formation assays indicated that overexpression of circFAT1(e2) in MGC-803 and MKN-28 cells could significantly reduce the colony number, however, YBX1 could abolish the reduction of colonies induced by circFAT1(e2) overexpression (Fig. 7E and F). These findings demonstrated that circFAT1(e2) could inhibit GC cell proliferation through YBX1.

4. Discussion

Despite the rapid advancement of early diagnosis and therapy in GC, most GC patients inevitably progress to an advanced stage, which is characterized by metastatic and chemo-resistant disease [5,19]. During the last few years, scientists have realized that screening effective new biomarkers and exploring the signaling pathways associated with GC initiation and progression are extremely important for improving the prognosis of GC patients. In this study, we focused on circFAT1(e2), which was identified by circRNAs microarray, and validated the downregulation of circFAT1(e2) in GC human tissue specimens and cell lines. Patients with high circFAT1(e2) expression showed a better prognosis. Mechanistic analysis demonstrated that overexpression of circFAT1(e2) inhibited the capacity of proliferation, invasion, and migration of GC cells by specifically binding miR-548g and releasing RUNX1. In addition, circFAT1(e2) could suppress GC growth by targeting YBX1.

The term “circRNA” was first proposed by Sanger in 1976 and then achieved more and more attention all over the world [20,21]. CircRNAs exist as an enigmatic type of ncRNAs with unclear functions in mammal cells, and frequently exhibit tissue or developmental-stage specific expression [22,23]. Due to their excellent conservatism and stability properties, circRNAs were considered to be a promising biomarker of tumors in precision medicine [24]. Although the exact functions of the majority of circRNAs remain undetermined, emerging evidence has revealed that circRNAs are involved in the development of multiple diseases, such as neurodegenerative disorders, metabolic disorders, and different types of cancer [25–27]. For example, Xijing He et al. have identified that circRNA-0008717 may serve as an oncogene by targeting miR-203 in osteosarcoma [28]. Wang J and Li H reported that knockdown of circ_0067934 significantly inhibited proliferation, invasion, and migration of human nonsmall cell lung cancer (NSCLC) cells [29]. Zhang and coworkers indicated that circular RNA_LARP4 inhibits cell proliferation and invasion of gastric cancer by sponging miR-424-5p and regulating LATS1 expression [30]. However, the exact role of circRNAs in GC remains largely unclear. In this study, a circRNA microarray analysis was carried out to examine the circRNA expression profiles of GC tissues and related normal tissues to investigate the correlation between circRNAs and GC. We found that circFAT1(e2) was significantly downregulated in GC tissues and cell lines, and Kaplan-Meier analysis indicated that circFAT1(e2) may be a promising prognostic biomarker for GC patients. CircFAT1(e2) originates from exon 2 of the FAT1 gene and is distributed in both the cytoplasm and nucleus of GC cells. Moreover, we demonstrated that overexpression of circFAT1(e2) suppressed cell proliferation, migration, and invasion, implying that circFAT1(e2) may play as a tumor suppressor in GC.

MiRNAs, characterized by short sequence (~22 nt), are an abundant type of ncRNAs without protein encoding ability [31]. Previously, studies have revealed that miRNAs may bind to the 3′-untranslated

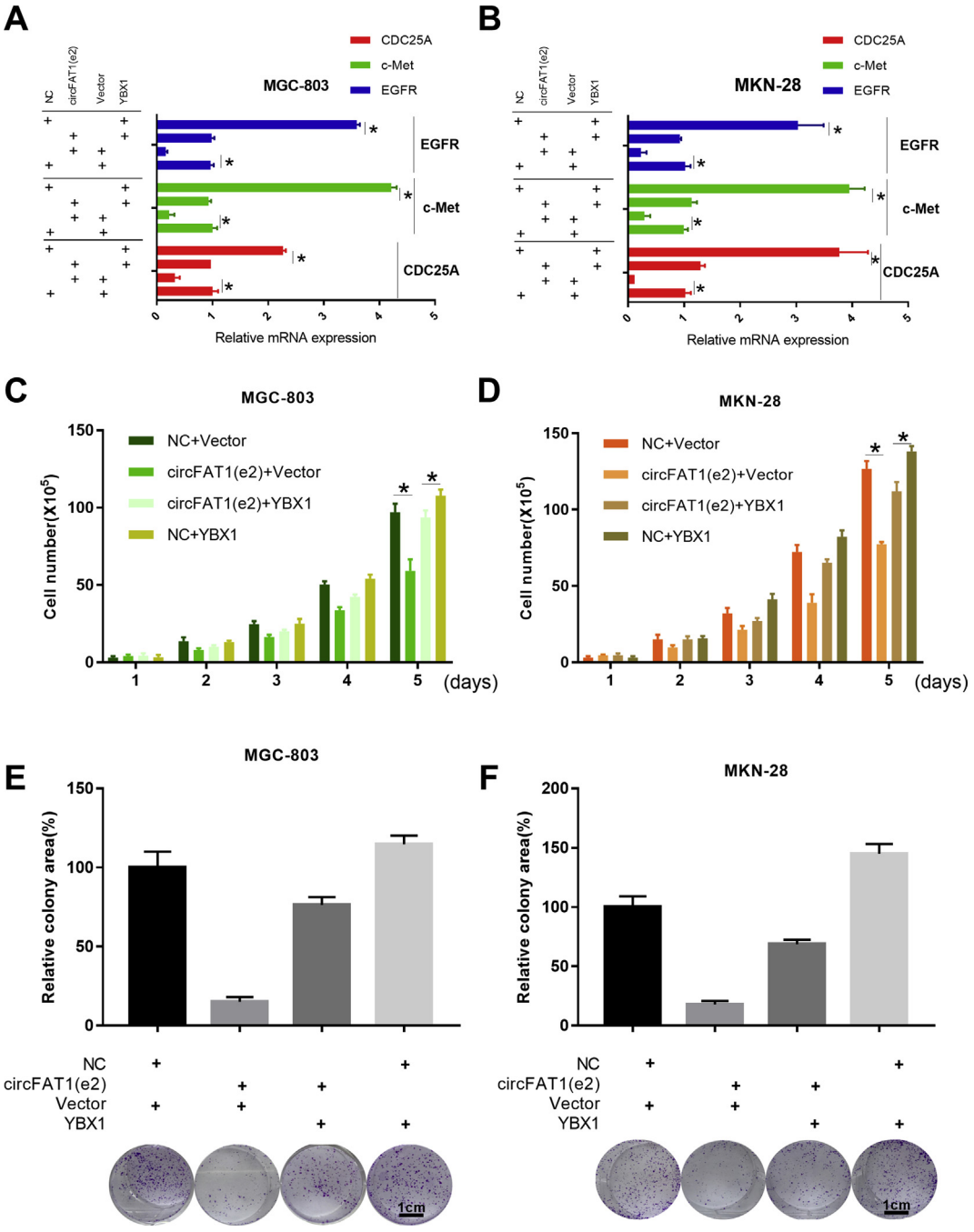

Fig. 7. circFAT1(e2) inhibited GC cell tumorigenesis through YBX1. (A and B) Relative mRNA expression of three targeted genes of YBX1 (EGFP, c-Met, and CDC25A) were measured by RT-PCR in MGC-803 and MKN-28 cells treated with circFAT1(e2) or YBX1. **(C and D)** Cell number of MGC-803 and MKN-28 cells treated with circFAT1(e2) or YBX1 were evaluated by MTT assay at 1, 2, 3, 4, and 5 days after transfection. **(E and F)** Colony formation assay was carried out to examine cell proliferation in MGC-803 and MKN-28 cells treated with circFAT1(e2) or YBX1.

regions (3′-UTR) of targeted mRNAs using miRNA response elements (MRE) to exhibit their posttranscriptional regulatory effects [32]. Computational searches performed in circRNAs for miRNAs binding sites revealed that many circRNAs contain MREs, indicating that circRNAs may act as miRNAs sponge, decreasing the miRNAs levels and releasing the targeted genes of miRNAs indirectly [33,34]. By performing a bioinformatics analysis and dual-luciferase reporter assay, we revealed and validated that circFAT1(e2) reduced the miR-548g levels by directly binding to it. To our best knowledge, this is the first report of miR-548g involvement in the progression of GC. We also found that RUNX1 was the targeted gene of miR-548g by bioinformatics analysis and dual-luciferase reporter assay. Additionally, RUNX1 could abolish the oncogenic effect of miR-548g. These results suggested that circFAT1(e2) in the cytoplasm inhibited GC progression by reducing the miR-548g levels and then releasing the targeted gene of miR-548g RUNX1. RUX1, an important tumor suppressor and transcription factor, was reported to inhibit GC progression [35,36], which was consistent with our results.

In addition, we investigated the functions of circFAT1(e2) in the nucleus by performing the online catRAPID analysis and circRIP assay. The results showed that circFAT1(e2) may directly interact with YBX1 and the tumor suppressive effect of circFAT1(e2) was abolished by YBX1. YBX1, which belongs to the DNA- and RNA-binding protein family, was demonstrated to be a potential biomarker in GC diagnosis

[37]. Furthermore, knockdown of the YBX1 gene suppressed cell migration of GC cells *in vitro* [38], indicating that YBX1 served as an oncogenic agent in GC, which was also consistent with our findings.

In conclusion, we revealed that circFAT1(e2) acted as a tumor suppressor in GC by reducing the miR-548g levels in the cytoplasm, and subsequently releasing the miR-548g targeted gene RUNX1. Meanwhile, circFAT1(e2) in the nucleus could bind to the YBX1 protein to inhibit GC progression. However, further analyses needed to be combined to obtain a larger number of circRNAs in GC. Moreover, it will be necessary to explore the deeper mechanisms of circFAT1(e2) in GC.

Disclosure of potential conflicts of interest

The authors declare no potential conflicts of interest.

Conflicts of interest

The authors have no commercial or other associations that might pose a conflict of interest.

Acknowledgments

This work was supported by the National Youthful Science Foundation of China (Nos. 81302145) and the Science and Technology Research Project of the Science and Technology Bureau of Suzhou City (Nos. SYS201330).

Appendix A. Supplementary data

Supplementary data to this article can be found online at https://doi.org/10.1016/j.canlet.2018.10.040.

References

[1] P. Karimi, F. Islami, S. Anandasabapathy, N.D. Freedman, F. Kamangar, Gastric cancer: descriptive epidemiology, risk factors, screening, and prevention, Cancer Epidemiol. Biomark. Prev. 23 (2014) 700–713.
[2] M. Abbas, A. Faggian, D.N. Sintali, G.J. Khan, S. Naeem, M. Shi, C. Dingding, Current and future biomarkers in gastric cancer, Biomed. Pharmacother. 103 (2018) 1688–1700.
[3] J. Ferlay, E. Steliarova-Foucher, J. Lortet-Tieulent, S. Rosso, J.W. Coebergh, H. Comber, D. Forman, F. Bray, Cancer incidence and mortality patterns in Europe: estimates for 40 countries in 2012, Eur. J. Canc. 49 (2013) 1374–1403.
[4] R. Herrero, J.Y. Park, D. Forman, The fight against gastric cancer - the IARC Working Group report, Best Pract. Res. Clin. Gastroenterol. 28 (2014) 1107–1114.
[5] H.M. Dong, Q. Wang, W.L. Wang, G. Wang, X.K. Li, G.D. Li, J. Chen, A clinical analysis of systemic chemotherapy combined with radiotherapy for advanced gastric cancer, Medicine (Baltim.) 97 (2018) e10786.
[6] V.S. Patil, R. Zhou, T.M. Rana, Gene regulation by non-coding RNAs, Crit. Rev. Biochem. Mol. Biol. 49 (2014) 16–32.
[7] Z. Strmsek, T. Kunej, MicroRNA silencing by DNA methylation in human cancer: a literature analysis, Noncoding RNA 1 (2015) 44–52.
[8] C.H. Li, Y. Chen, Targeting long non-coding RNAs in cancers: progress and prospects, Int. J. Biochem. Cell Biol. 45 (2013) 1895–1910.
[9] M.U. Kaikkonen, M.T. Lam, C.K. Glass, Non-coding RNAs as regulators of gene expression and epigenetics, Cardiovasc. Res. 90 (2011) 430–440.
[10] L. Comai, B. Zhang, MicroRNAs: key gene regulators with versatile functions, Plant Mol. Biol. 80 (2012) 1.
[11] X. Bai, G. Han, Y. Liu, H. Jiang, Q. He, MiRNA-20a-5p promotes the growth of triple-negative breast cancer cells through targeting RUNX3, Biomed. Pharmacother. 103 (2018) 1482–1489.
[12] miRNA-124 down-regulates SOX8 expression and suppresses cell proliferation in non-small cell lung cancer [Retraction], Int. J. Clin. Exp. Pathol. 9 (2016) 2756.
[13] Z. Chen, X. Zuo, Y. Zhang, G. Han, L. Zhang, J. Wu, X. Wang, MiR-3662 suppresses hepatocellular carcinoma growth through inhibition of HIF-1alpha-mediated Warburg effect, Cell Death Dis. 9 (2018) 549.
[14] J. Li, J. Yang, P. Zhou, Y. Le, C. Zhou, S. Wang, D. Xu, H.K. Lin, Z. Gong, Circular RNAs in cancer: novel insights into origins, properties, functions and implications, Am. J. Canc. Res. 5 (2015) 472–480.
[15] Z. Wu, W. Shi, C. Jiang, Overexpressing circular RNA hsa_circ_0002052 impairs osteosarcoma progression via inhibiting Wnt/beta-catenin pathway by regulating miR-1205/APC2 axis, Biochem. Biophys. Res. Commun. 502 (4) (2018) 465–471.
[16] X. Zhang, P. Luo, W. Jing, H. Zhou, C. Liang, J. Tu, circSMAD2 inhibits the epithelial-mesenchymal transition by targeting miR-629 in hepatocellular carcinoma, OncoTargets Ther. 11 (2018) 2853–2863.
[17] P. Li, X. Yang, W. Yuan, C. Yang, X. Zhang, J. Han, J. Wang, X. Deng, H. Yang, P. Li, J. Tao, Q. Lu, M. Gu, CircRNA-Cdr1as exerts anti-oncogenic functions in bladder cancer by sponging MicroRNA-135a, Cell. Physiol. Biochem. 46 (2018) 1606–1616.
[18] Y. Chen, M.C. Lin, H. Yao, H. Wang, A.Q. Zhang, J. Yu, C.K. Hui, G.K. Lau, M.L. He, J. Sung, H.F. Kung, Lentivirus-mediated RNA interference targeting enhancer of zeste homolog 2 inhibits hepatocellular carcinoma growth through down-regulation of stathmin, Hepatology 46 (2007) 200–208.
[19] S. Matsui, M. Kudo, M. Kitano, Y. Asakuma, Evaluation of the response to chemotherapy in advanced gastric cancer by contrast-enhanced harmonic EUS, Hepato-Gastroenterology 62 (2015) 595–598.
[20] H.L. Sanger, G. Klotz, D. Riesner, H.J. Gross, A.K. Kleinschmidt, Viroids are single-stranded covalently closed circular RNA molecules existing as highly base-paired rod-like structures, Proc. Natl. Acad. Sci. U. S. A. 73 (1976) 3852–3856.
[21] K. Lei, H. Bai, Z. Wei, C. Xie, J. Wang, J. Li, Q. Chen, The mechanism and function of circular RNAs in human diseases, Exp. Cell Res. 368 (2018) 147–158.
[22] B.J. Chen, S. Huang, M. Janitz, Changes in Circular RNA Expression Patterns during Human Foetal Brain Development, Genomics, 2018.
[23] Y. Shao, J. Li, R. Lu, T. Li, Y. Yang, B. Xiao, J. Guo, Global circular RNA expression profile of human gastric cancer and its clinical significance, Canc. Med. 6 (2017) 1173–1180.
[24] S. Qu, X. Yang, X. Li, J. Wang, Y. Gao, R. Shang, W. Sun, K. Dou, H. Li, Circular RNA: a new star of noncoding RNAs, Cancer Lett. 365 (2015) 141–148.
[25] L. Kumar, Shamsuzzama, R. Haque, T. Baghel, A. Nazir, Circular RNAs: the emerging class of non-coding RNAs and their potential role in human neurodegenerative diseases, Mol. Neurobiol. 54 (2017) 7224–7234.
[26] Z. Zhao, X. Li, D. Jian, P. Hao, L. Rao, M. Li, Hsa_circ_0054633 in peripheral blood can be used as a diagnostic biomarker of pre-diabetes and type 2 diabetes mellitus, Acta Diabetol. 54 (2017) 237–245.
[27] J.J. Chan, Y. Tay, Noncoding RNA:RNA regulatory networks in cancer, Int. J. Mol. Sci. 19 (2018).
[28] X. Zhou, D. Natino, Z. Qin, D. Wang, Z. Tian, X. Cai, B. Wang, X. He, Identification and functional characterization of circRNA-0008717 as an oncogene in osteosarcoma through sponging miR-203, Oncotarget 9 (2018) 22288–22300.
[29] J. Wang, H. Li, CircRNA circ_0067934 silencing inhibits the proliferation, migration and invasion of NSCLC cells and correlates with unfavorable prognosis in NSCLC, Eur. Rev. Med. Pharmacol. Sci. 22 (2018) 3053–3060.
[30] J. Zhang, H. Liu, L. Hou, G. Wang, R. Zhang, Y. Huang, X. Chen, J. Zhu, Circular RNA_LARP4 inhibits cell proliferation and invasion of gastric cancer by sponging miR-424-5p and regulating LATS1 expression, Mol. Canc. 16 (2017) 151.
[31] Y. Tutar, miRNA and cancer; computational and experimental approaches, Curr. Pharm. Biotechnol. 15 (2014) 429.
[32] D.P. Bartel, MicroRNAs: target recognition and regulatory functions, Cell 136 (2009) 215–233.
[33] S. Memczak, M. Jens, A. Elefsinioti, F. Torti, J. Krueger, A. Rybak, L. Maier, S.D. Mackowiak, L.H. Gregersen, M. Munschauer, A. Loewer, U. Ziebold, M. Landthaler, C. Kocks, F. le Noble, N. Rajewsky, Circular RNAs are a large class of animal RNAs with regulatory potency, Nature 495 (2013) 333–338.
[34] W.W. Du, W. Yang, E. Liu, Z. Yang, P. Dhaliwal, B.B. Yang, Foxo3 circular RNA retards cell cycle progression via forming ternary complexes with p21 and CDK2, Nucleic Acids Res. 44 (2016) 2846–2858.
[35] N. Li, Q.Y. Zhang, J.L. Zou, Z.W. Li, T.T. Tian, B. Dong, X.J. Liu, S. Ge, Y. Zhu, J. Gao, L. Shen, miR-215 promotes malignant progression of gastric cancer by targeting RUNX1, Oncotarget 7 (2016) 4817–4828.
[36] G. Liu, T. Xiang, Q.F. Wu, W.X. Wang, Long noncoding RNA H19-derived miR-675 enhances proliferation and invasion via RUNX1 in gastric cancer cells, Oncol. Res. 23 (2016) 99–107.
[37] Z. Zhang, M. Dou, X. Yao, H. Tang, Z. Li, X. Zhao, Potential biomarkers in diagnosis of human gastric cancer, Canc. Invest. 34 (2016) 115–122.
[38] T.T. Guo, Y.N. Yu, G.W. Yip, K. Matsumoto, B.H. Bay, Silencing the YB-1 gene inhibits cell migration in gastric cancer in vitro, Anat. Rec. 296 (2013) 891–898.